Inorg. Chem. **2005**, *44*, 1601−1610

Two Stereoisomers of an S-Bridged $Rh^{III}_2Pt^{II}_2$ Tetranuclear Complex $[\{Pt(NH_3)_2\}_2\{Rh(aet)_3\}_2]^{4+}$ That Lead to a Discrete and a 1D $Rh^{III}_2Pt^{II}_2Ag^{I}$ Structures by Reacting with Ag^{I} (aet = 2-Aminoethanethiolate)

Yu Chikamoto, Tatsuya Kawamoto, Asako Igashira-Kamiyama, and Takumi Konno*

Department of Chemistry, Graduate School of Science, Osaka University, Toyonaka, Osaka 560-0043, Japan

Received September 20, 2004

An S-bridged $Rh^{III}_2Pt^{II}_2$ tetranuclear complex having two nonbridging thiolato groups, $[\{Pt(NH_3)_2\}_2\{Rh(aet)_3\}_2]^{4+}$ ($[\mathbf{1}]^{4+}$), in which two *fac*(*S*)-$[Rh(aet)_3]$ units are linked by two *trans*-$[Pt(NH_3)_2]^{2+}$ moieties, was synthesized by the 1:1 reaction of *fac*(*S*)-$[Rh(aet)_3]$ (aet = 2-aminoethanethiolate) with *trans*-$[PtCl_2(NH_3)_2]$ in water. Complex $[\mathbf{1}]^{4+}$ gave both the *meso* ($\Delta\Lambda$) and *racemic* ($\Delta\Delta/\Lambda\Lambda$) forms, which were separated by fractional crystallization. Of two possible geometries, *syn* and *anti*, which arise from the arrangement of two nonbridging thiolato groups, the *meso* and *racemic* forms of $[\mathbf{1}]^{4+}$ selectively afforded the *anti* and *syn* geometries, respectively. The $\Delta\Lambda$-*anti* and $\Delta\Delta/\Lambda\Lambda$-*syn* isomers of $[\mathbf{1}]^{4+}$ reacted with Ag^+ using two nonbridging thiolato groups to produce a $\{Rh^{III}_2Pt^{II}_2Ag^{I}\}_n$ polymeric complex, $\{[Ag\{Pt(NH_3)_2\}_2\{Rh(aet)_3\}_2]^{5+}\}_n$ ($[\mathbf{2}]^{5+}$), and a $Rh^{III}_2Pt^{II}_2Ag^{I}$ pentanuclear complex, $[Ag\{Pt_2(\mu\text{-}H_2O)(NH_3)_2\}\{Rh(aet)_3\}_2]^{5+}$ ($[\mathbf{3}]^{5+}$), respectively, which contain octahedral Rh^{III}, square-planar Pt^{II}, and linear Ag^{I} centers. In $[\mathbf{2}]^{5+}$, each $\Delta\Lambda$-*anti*-$[\{Pt(NH_3)_2\}_2\{Rh(aet)_3\}_2]^{4+}$ tetranuclear unit is bound to two Ag^{I} atoms to form a one-dimensional zigzag chain, indicating the retention of the parental S-bridged structure in $\Delta\Lambda$-*anti*-$[\mathbf{1}]^{4+}$. In $[\mathbf{3}]^{5+}$, two Δ- or Λ-*fac*(*S*)-$[Rh(aet)_3]$ units are linked by a $[Pt_2(\mu\text{-}H_2O)(NH_3)_2]^{4+}$ dinuclear moiety, together with an Ag^{I} atom, indicating that two NH_3 molecules in $[\mathbf{1}]^{4+}$ have been replaced by a water molecule that bridges two Pt^{II} centers, while the parental $\Delta\Delta/\Lambda\Lambda$-*syn* configuration is retained. The complexes obtained were characterized on the basis of electronic absorption, CD, and NMR spectra, along with single-crystal X-ray analyses.

Introduction

The self-assembly process has attracted much interest as a rational and useful means to construct a variety of metallo-supramolecular architectures.[1] A large number of metallo-supramolecules have been prepared through this process, using multidentate organic ligands and selected metal ions, which serve as a building block and a linking unit, respectively. On the other hand, examples of the use of metal complexes having several binding sites with metal ions as a building block are relatively rare. For the purpose of the rational construction of polynuclear and polymeric metallo-supramolecular structures, our interest has been directed toward the assembly of octahedral metal complexes with thiolate-type chelating ligands, such as 2-aminoethanthiolate (aet), L-cysteinate (L-cys), and D-penicillaminate (D-pen).[2] It has been shown that these metal complexes are readily aggregated by forming S-bridged structures with certain metal ions owing to the relatively high nucleophilicity of coordinated thiolato groups, resulting in the formation of polynuclear structures that are highly dependent on the coordination geometry of the reacting metal ions.[3]

In the course of studying the assembly of *fac*(*S*)-$[M(aet)_3]$ units ($M = Co^{III}$, Rh^{III}, Ir^{III}) assisted by transition metal ions, we recently found that the 2:1 reactions of *fac*(*S*)-$[Co(aet)_3]$

* To whom correspondence should be addressed. E-mail: konno@ch.wani.osaka-u.ac.jp.

(1) (a) Lehn, J. M. *Supramolecular Chemistry: Concepts and Perspectives*; VCH: Weinheim, 1995. (b) Leininger, S.; Olenyuk, B.; Stang, P. J. *Chem. Rev.* **2000**, *100*, 853−908. (c) Swiegers, G. F.; Malefetse, T. J. *Chem. Rev.* **2000**, *100*, 3483−3537. (d) Holliday, B. J.; Mirkin, C. A *Angew. Chem., Int. Ed.* **2001**, *40*, 2022−2043. (e) Ward, M. D.; McCleverty, J. A.; Jeffery J. C. *Coord. Chem. Rev.* **2001**, *222*, 251−272. (f) Janiak, C. *Dalton Trans.* **2003**, 2781−2804.

(2) (a) Konno, T.; Yoshimura, T.; Aoki, K.; Okamoto, K.; Hirotsu, M. *Angew. Chem., Int. Ed.* **2001**, *40*, 1765−1768. (b) Konno, T.; Yoshimura, T.; Masuyama, G.; Hirotsu, M.; *Bull. Chem. Soc. Jpn.* **2002**, *75*, 2185−2193. (c) Konno, T.; Shimazaki, Y.; Yamaguchi, T.; Ito, T.; Hirotsu, M. *Angew. Chem., Int. Ed.* **2002**, *41*, 4711−4715. (d) Hirotsu, M.; Kobayashi, A.; Yoshimura, T.; Konno, T. *J. Chem. Soc., Dalton Trans.* **2002**, 878−884.

(3) Konno, T. *Bull. Chem. Soc. Jpn.* **2004**, *77*, 627−649.

10.1021/ic048680k CCC: $30.25
Published on Web 01/26/2005

with $[PdCl_4]^{2-}$ are accompanied by the isomerization of *fac*(*S*) to *mer*(*S*) to afford an S-bridged $Co^{III}PdCo^{III}$ trinuclear complex having two nonbridging thiolato groups, $[Pd\{Co(aet)_3\}_2]^{2+}$.[4] Furthermore, $[Pd\{Co(aet)_3\}_2]^{2+}$ was found to bind with linear metal ions (M = Ag^I, Au^I) through nonbridging thiolato groups to form S-bridged $Co^{III}_4Pd^{II}_2M_2$ octanuclear metallacycles, $[M_2\{Pd\{Co(aet)_3\}_2\}_2]^{6+}$.[4] This result indicated that S-bridged polynuclear complexes with nonbridging thiolato groups could be used as a building block for the construction of heterometallic supramolecular aggregates. Thus, our effort was focused on the preparation of novel S-bridged polynuclear complexes of this class based on *fac*(*S*)-$[Rh(aet)_3]$, which is much more robust than *fac*(*S*)-$[Co(aet)_3]$,[3] so that the *fac*(*S*) geometry should be retained. Previous attempts to prepare an S-bridged $Rh^{III}Pd^{II}Rh^{III}$ trinuclear complex, analogous to $[Pd\{Co(aet)_3\}_2]^{2+}$, by the reaction of *fac*(*S*)-$[Rh(aet)_3]$ with $[PdCl_4]^{2-}$ were unsuccessful, forming uncharacterized polymeric species at room temperature and an S-bridged $Rh^{III}_3Pd^{II}_2$ pentanuclear $[Pd\{Pd(aet)\}\{Rh(aet)_2\}\{Rh(aet)_3\}_2]^{4+}$ at a high temperature.[3,5] This was also the case for the reactions of *fac*(*S*)-$[Rh(aet)_3]$ with $[PtCl_4]^{2-}$. However, the use of *trans*-$[PtCl_2(NH_3)_2]$, instead of $[PdCl_4]^{2-}$ or $[PtCl_4]^{2-}$, was found to produce a desired $Rh^{III}_2Pt^{II}_2$ tetranuclear complex, $[\{Pt(NH_3)_2\}_2\{Rh(aet)_3\}_2]^{4+}$ ($[\mathbf{1}]^{4+}$), which possesses two nonbridging thiolato groups.

In this paper, we report on the synthesis, characterization, and stereochemistry of $[\mathbf{1}]^{4+}$ (Scheme 1). The isomers formed for $[\mathbf{1}]^{4+}$ were separated and then reacted with Ag^I ion to obtain S-bridged polynuclear species with a higher nuclearity. The crystal structures of the isomers of $[\mathbf{1}]^{4+}$, together with their Ag^I adducts, are also reported. While the aggregation of thiolato metal complexes has been extensively performed in combination with linear transition metal ions,[2b,3,6] the present study first shows the utility of *trans*-$[Pt(NH_3)_2]$ unit as an effective linear-type linker for the construction of novel S-bridged polynuclear and polymeric structures.

Scheme 1

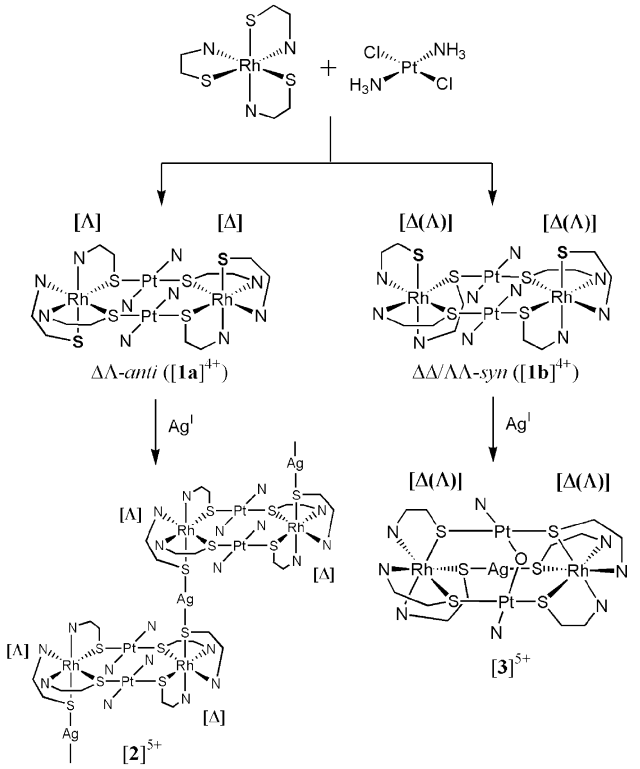

Experimental Section

Preparation and Separation of ΔΛ-*anti*-[{Pt(NH$_3$)$_2$}$_2${Rh(aet)$_3$}$_2$](NO$_3$)$_4$ ([1a](NO$_3$)$_4$) and ΔΔ/ΛΛ-*syn*-[{Pt(NH$_3$)$_2$}$_2${Rh(aet)$_3$}$_2$](NO$_3$)$_4$ ([1b] (NO$_3$)$_4$). To a yellow suspension containing *fac*(*S*)-$[Rh(aet)_3]$[7] (0.50 g, 1.51 mmol) in 50 cm^3 of water was added *trans*-$[PtCl_2(NH_3)_2]$[8] (0.50 g, 1.67 mmol). The mixture was stirred at 0 °C for 12 h, during which time the suspension turned to a yellow solution. After unreacted materials were filtered off, to the filtrate was added 5 cm^3 of a saturated $NaNO_3$ aqueous solution, followed by standing at room temperature for 3 days. The resulting yellow crystalline solid of [**1a**](NO$_3$)$_4$ was collected by filtration and then recrystallized from a small amount of water at room temperature to give yellow plate crystals suitable for X-ray analysis. When the remaining filtrate was allowed to stand at 4 °C for 3 days, a yellow powder of [**1b**](NO$_3$)$_4$ appeared, which was collected by filtration and recrystallized from a small amount of water by adding a saturated $NaNO_3$ aqueous solution. Yield for [**1a**](NO$_3$)$_4$: 0.32 g (29%). Anal. Calcd for $[\{Pt(NH_3)_2\}_2\{Rh(C_6H_{18}N_3S_3)\}_2](NO_3)_4\cdot 6H_2O$: C, 9.76; H, 4.09; N, 13.28%. Found: C, 9.92; H, 3.85; N, 13.42%. ^{13}C NMR (D_2O): δ 31.87 ($-CH_2S$), 33.14 ($-CH_2S$), 36.62 ($-CH_2S$), 47.87 ($-CH_2NH_2$), 49.20 ($-CH_2NH_2$), 51.26 ($-CH_2NH_2$). ^{195}Pt NMR (D_2O): δ −2839. Molar conductivity in H_2O: 501 Ω^{-1} cm^2 mol^{-1}. IR (Nujol, cm^{-1}): 1591 s br, 1048 m, 1135 w, 982 s, 924 w, 853 m, 824 m, 721 m. Yield for [**1b**](NO$_3$)$_4$: 0.20 g (18%). Anal. Calcd for $[\{Pt(NH_3)_2\}_2\{Rh(C_6H_{18}N_3S_3)\}_2](NO_3)_4\cdot 6H_2O$: C, 9.76; H, 4.09; N, 13.28%. Found: C, 9.74; H, 3.86; N, 13.30%. ^{13}C NMR (D_2O): δ 32.86 ($-CH_2S$), 32.92 ($-CH_2S$), 36.84 ($-CH_2S$), 47.88 ($-CH_2NH_2$), 49.27 ($-CH_2NH_2$), 51.19 ($-CH_2NH_2$). ^{195}Pt NMR (D_2O): δ −2820. Molar conductivity in H_2O: 509 Ω^{-1} cm^2 mol^{-1}. IR (Nujol, cm^{-1}): 1576 s br, 1135 w, 1048 m, 980 s, 924 w, 853 m, 824 m, 723 m. Yellow needle crystals of [**1b**](ClO$_4$)$_4\cdot$2H$_2$O suitable for X-ray analysis were obtained by the metathesis of [**1b**](NO$_3$)$_4$ with $NaClO_4$ in water, followed the recrystallization from a small amount of water at room temperature.

An aqueous solution of [**1b**](NO$_3$)$_4$ was chromatographed on an SP−Sephadex C-25 column (Na^+ form, 2 cm × 30 cm), using a 0.4 mol dm^{-3} aqueous solution of $Na_2[Sb_2(R,R\text{-tartrato})_2]\cdot 5H_2O$ as an eluent. When the developed band was completely separated into two bands in the column, the eluent was changed to a 0.8 mol dm^{-3} aqueous solution of $NaNO_3$. Each eluate of the two bands was concentrated to a small volume, and the concentrate was used for the CD spectral measurement. The concentration of each eluate

(4) Konno, T.; Chikamoto, Y.; Okamoto, K.; Yamaguchi, T.; Ito, T.; Hirotsu, M. *Angew. Chem., Int. Ed.* **2000**, *39*, 4098−4101.
(5) (a) Konno, T.; Sasaki, C.; Okamoto, K. *Chem. Lett.* **1996**, 977−978. (b) Okamoto, K.; Sasaki, C.; Yamada, Y.; Konno, T. *Bull. Chem. Soc. Jpn.* **1999**, *72*, 1685−1696.
(6) (a) Heeg, M. J.; Elder, R. C.; Deutsch, E. *Inorg. Chem.* **1980**, *19*, 554−556. (b) Birker, P. J. M. W. L.; Verschoor, G. C. *Inorg. Chem.* **1982**, *21*, 990−995. (c) Vicente, J.; Chicote, M. T.; Huertas, S.; Bautista, D. *Inorg. Chem.* **2001**, *40*, 2051−2057. (d) Konno, T.; Hattori, M.; Yoshimura, T.; Hirotsu, M. *Chem. Lett.* **2002**, 852−853. (e) Konno, T.; Hattori, M.; Yoshimura, T.; Hirotsu, M. *Chem. Lett.* **2002**, 230−231. (f) Rao, P. V.; Bhaduri, S.; Jiang, J.; Holm, R. H.; *Inorg. Chem.* **2004**, *43*, 5833−5849.
(7) Konno, T.; Okamoto, K.; Hidaka, J. *Inorg. Chem.* **1994**, *33*, 538−544.
(8) Kauffman, G. B.; Cowan, D. O. *Inorg. Synth.* **1963**, *7*, 239−245.

Table 1. Crystallographic Data of Complexes

	[**1a**]$(NO_3)_4$·$6H_2O$	[**1b**]$(ClO_4)_4$·$2H_2O$	[**2**]$(ClO_4)_5$·$3H_2O$	[**3**]$(NO_3)_5$·$10H_2O$
empirical formula	$C_{12}H_{60}N_{14}O_{18}Pt_2Rh_2S_6$	$C_{12}H_{52}N_{10}Cl_4O_{18}Pt_2Rh_2S_6$	$C_{12}H_{54}N_{10}Ag_1Cl_5Rh_2O_{23}Pt_2S_6$	$C_{12}H_{64}N_{13}Ag_1O_{26}Pt_2Rh_2S_6$
fw	1477.10	1554.78	1780.14	1702.99
space group	$P\bar{1}$	$P\bar{1}$	$P2_1/n$	$P2_1/n$
a, Å	8.766(2)	14.423(3)	11.747(5)	16.424(11)
b, Å	9.003(2)	18.010(3)	12.619(8)	14.923(9)
c, Å	14.400(3)	8.903(6)	16.134(10)	19.189(12)
α, deg	78.99(2)	103.89(3)		
β, deg	83.48(1)	93.10(3)	102.99(5)	96.14(6)
γ, deg	71.50(1)	98.12(1)		
V, Å^3	1059.8(3)	2213(2)	2331(2)	4676(5)
Z	1	2	2	4
T, K	296	298	200	200
radiation *λ*, Å	0.7107	0.7107	0.7107	0.7107
ρ_{calcd}, cm^{-3}	2.314	2.279	2.537	2.419
μ(Mo Kα), cm^{-1}	7.719	7.671	7.727	7.426
R	0.030	0.073	0.078	0.044
R_w	0.074	0.089	0.143	0.065

was evaluated on the basis of the absorption spectral data of the *racemic* nitrate salt. It was found from the absorption and CD spectral measurements that the earlier and the later moving bands in the column contained the $(+)^{CD}_{380}$ and $(-)^{CD}_{380}$ isomers, respectively.

Preparation of {[Ag{Pt(NH$_3$)$_2$}$_2${Rh(aet)$_3$}$_2$](ClO$_4$)$_5$}$_n$ ([2](ClO$_4$)$_5$). To a yellow solution containing ΔΛ-*anti*-[{Pt(NH$_3$)$_2$}$_2$-{Rh(aet)$_3$}$_2$](NO$_3$)$_4$·6H$_2$O (0.07 g, 0.05 mmol) in 20 cm^3 of water was added a solution containing $AgClO_4$ (0.01 g, 0.05 mmol) in 1 cm^3 of water. The mixture was stirred at 60 °C for 30 min, and then several drops of a saturated $NaClO_4$ aqueous solution were added to it. The mixture solution was allowed to stand at room temperature for 5 days, and the resulting yellow plate crystals suitable for X-ray analysis were collected by filtration. Yield: 0.07 g (83%). Anal. Calcd for [Ag{Pt(NH$_3$)$_2$}$_2${Rh(C$_6$H$_{18}$N$_3$S$_3$)}$_2$](ClO$_4$)$_5$·3H$_2$O: C, 8.10; H, 3.06; N, 7.87. Found: C, 8.23; H, 2.95; N, 7.90. IR (Nujol, cm^{-1}): 1576 m br, 1328 m br, 1238 m, 1058 s br, 977 w, 924 w, 849 m, 721 w, 623 m.

Preparation and Optical Resolution of [Ag{Pt$_2$(H$_2$O)(NH$_3$)$_2$}-{Rh(aet)$_3$}$_2$](NO$_3$)$_5$ ([3](NO$_3$)$_5$). To a yellow solution containing ΔΔ/ΛΛ-*syn*-[{Pt(NH$_3$)$_2$}$_2${Rh(aet)$_3$}$_2$](NO$_3$)$_4$·6H$_2$O (0.07 g, 0.05 mmol) in 20 cm^3 of water was added a solution containing $AgNO_3$ (0.01 g, 0.06 mmol) in 1 cm^3 of water. The mixture was stirred at room temperature for 3 h, and then several drops of a saturated $NaNO_3$ aqueous solution were added to it. The mixture solution was allowed to stand at 4 °C for 8 days, and the resulting yellow powder was collected by filtration. This powder was recrystallized from a small amount of water by adding a saturated $NaNO_3$ aqueous solution to give yellow plate crystals suitable for X-ray analysis. Yield: 0.04 g (52%). Anal. Calcd for [Ag{Pt$_2$(H$_2$O)(NH$_3$)$_2$}{Rh-(C$_6$H$_{18}$N$_3$S$_3$)}$_2$](NO$_3$)$_5$·5H$_2$O: C, 8.94; H, 3.37; N, 11.29. Found: C, 8.85; H, 3.56; N, 11.19. ^{13}C NMR (D$_2$O): δ 34.34 (−CH$_2$S), 35.77 (−CH$_2$S), 38.98 (−CH$_2$S), 49.05 (−CH$_2$NH$_2$), 49.76 (−CH$_2$-NH$_2$), 51.04 (−CH$_2$NH$_2$). ^{195}Pt NMR (D$_2$O): δ −2885. Molar conductivity in H$_2$O: 601 Ω^{-1} cm^2 mol^{-1}. IR (Nujol, cm^{-1}): 1576 m br, 1328 s br, 1125 w, 1044 s, 980 s, 920 w, 853 w, 822 m, 723 m.

An aqueous solution of [**3**](NO$_3$)$_5$ was chromatographed on an SP−Sephadex C-25 column (Na$^+$ form, 2 cm × 30 cm), using a 0.4 mol dm^{-3} aqueous solution of Na$_2$[Sb$_2$(*R*,*R*-tartrato)$_2$]·5H$_2$O as an eluent. When the developed band was completely separated into two bands in the column, the eluent was changed to a 0.8 mol dm^{-3} aqueous solution of $NaNO_3$. Each eluate of the two bands was concentrated to a small volume, and the concentrate was used for the CD spectral measurement. The concentration of each eluate was evaluated on the basis of the absorption spectral data of the *racemic* nitrate salt. It was found from the absorption and CD spectral measurements that the earlier and the later moving bands in the column contained the $(+)^{CD}_{380}$ and $(-)^{CD}_{380}$ isomers, respectively.

Caution! Perchlorate salts of metal complexes are potentially explosive and should be handled in small quantities.

Physical Measurements. The electronic absorption spectra were recorded on a Ubest-55 spectrophotometer and the CD spectra on a JASCO J-700 spectropolarimeter at room temperature. The elemental analyses (C, H, N) were performed by the Analysis Center of Osaka University. The X-ray fluorescence analyses were made on a HORIBA MESA-500 spectrometer. The ^{13}C NMR spectra were recorded on a JEOL JNM-A500 NMR spectrometer at the probe temperature in D$_2$O, using sodium 4,4-dimethyl-4-silapentane-1-sulfonate (DSS) as the internal reference. The ^{195}Pt NMR spectra were recorded on a Varian Unity plus-600 NMR spectrometer at the probe temperature in D$_2$O, using Na$_2$[PtCl$_6$] as the external reference. The molar conductivities of the complexes were measured with a HORIBA conductivity meter DS-12 in aqueous solution at room temperature.

X-ray Structural Determination. Single-crystal X-ray diffraction measurements for [**1a**](NO$_3$)$_4$·6H$_2$O and [**1b**](ClO$_4$)$_4$·2H$_2$O were made on a Rigaku AFC5R four-cycle diffractometer and a Mac Science MXC3 four-cycle diffractometer with a graphite monochromated Mo Kα radiation, respectively. Crystallographic data are summarized in Table 1. Unit cell parameters were determined by a least-squares refinement. The intensity data were collected by the $\omega-2\theta$ scan mode up to $2\theta = 60.1°$ for [**1a**](NO$_3$)$_4$·6H$_2$O and by the $\theta-2\theta$ scan mode up to $2\theta = 52.9°$ for [**1b**](ClO$_4$)$_4$·2H$_2$O. The intensities were corrected for Lorentz and polarization. Empirical absorption corrections based on ψ scans were also applied. The 5159 and 6147 independent reflections with $I > 2\sigma(I)$ of the measured 6198 and 7364 reflections were considered as "observed" and used for the structure determinations of [**1a**](NO$_3$)$_4$·6H$_2$O and [**1b**](ClO$_4$)$_4$·2H$_2$O, respectively. The structures were solved by direct methods and expanded using Fourier techniques. The non-hydrogen atoms were refined anisotropically by full-matrix least-squares methods. Hydrogen atoms except those of water molecules were placed at calculated positions but were not refined. All calculations for [**1a**](NO$_3$)$_4$·6H$_2$O and [**1b**]-(ClO$_4$)$_4$·2H$_2$O were performed using the CrystalStructure crystallographic software package and the Crystan-GM crystallographic software package, respectively.[9a,b]

Single-crystal X-ray diffraction measurements for [**2**]$(ClO_4)_5$·$3H_2O$ and [**3**]$(NO_3)_5$·$10H_2O$ were made on a imaging plate area detector with a loop wire monochromated Mo Kα radiation. Crystallographic data are summarized in Table 1. Unit cell parameters were determined by a least-squares refinement. The intensity data were collected by the ω scan mode up to $2\theta_{max} = 55.1°$ for [**2**]$(ClO_4)_5$·$3H_2O$ and to $2\theta_{max} = 55.3°$ for [**3**]$(NO_3)_5$·$10H_2O$. The intensities were corrected for Lorentz and polarization. Empirical absorption corrections were also applied. The 4064 and 8813 independent reflections with $I > 2\sigma(I)$ of the measured 5330 and 10612 reflections were considered as "observed" and used for the structure determinations of [**2**]$(ClO_4)_5$·$3H_2O$ and [**3**]$(NO_3)_5$·$10H_2O$, respectively. The structures were solved by direct methods and expanded using Fourier techniques. The non-hydrogen atoms were refined anisotropically by full-matrix least-squares methods. Hydrogen atoms except those of water molecules for [**2**]$(ClO_4)_5$·$3H_2O$ were placed at calculated positions but were not refined. For [**3**]$(NO_3)_5$·$10H_2O$ hydrogen atoms of amine groups and a bridging water molecule were found from difference Fourier maps, while other hydrogen atoms except those of solvated water molecules were placed at calculated positions but were not refined. Four of five nitrate anions, as well as solvated water molecules in [**3**]$(NO_3)_5$·$10H_2O$, were highly disordered and one of them could not be modeled. All calculations were performed using the Crystal Structure crystallographic software package.[9a]

Results and Discussion

Synthesis and Characterization of Two Isomers of [{Pt(NH$_3$)$_2$}$_2${Rh(aet)$_3$}$_2$]$^{4+}$ ([1a]$^{4+}$ and [1b]$^{4+}$). Treatment of an aqueous suspension of *fac*(*S*)-[Rh(aet)$_3$] with one molar equiv of *trans*-[$PtCl_2(NH_3)_2$] at 50 °C gave a clear, basic solution (pH ∼ 9.5) within 30 min, although each of *fac*(*S*)-[Rh(aet)$_3$] and [$PtCl_2(NH_3)_2$] is sparingly soluble in water. When this basic reaction solution was chromatographed on an SP−Sephadex C-25 cation-exchange column, little material was eluted even with a saturated aqueous solution of $NaNO_3$. Similar column chromatographic behavior has been recognized for the reaction solutions obtained from *fac*(*S*)-[Rh(aet)$_3$] and $[PdCl_4]^{2-}$ or $[PtCl_4]^{2-}$ at room temperature.[5] Thus, it is assumed that undesired $Rh^{III}Pt^{II}$ polymeric species, which are unidentified at present, are formed for the reaction of *fac*(*S*)-[Rh(aet)$_3$] with [$PtCl_2(NH_3)_2$] at a relatively high temperature because of the release of NH_3 molecules from [$PtCl_2(NH_3)_2$]. When an aqueous suspension of *fac*(*S*)-[Rh(aet)$_3$] was reacted with *trans*-[$PtCl_2(NH_3)_2$] at 0 °C, the suspension also turned to a clear solution (pH ∼ 6.0) after several hours, but its SP−Sephadex C-25 column chromatographic behavior was quite different. That is, a major yellow band of [**1**]$^{4+}$, which splits into two bands due to the diastereomers [**1a**]$^{4+}$ and [**1b**]$^{4+}$ in the column, was eluted with a 0.8 mol dm^{-3} aqueous solution of $NaNO_3$, while little was adsorbed on the top of the column. Compounds [**1a**]$^{4+}$ and [**1b**]$^{4+}$ were effectively separated and isolated as a nitrate salt directly from the reaction solution by fractional crystallization.

X-ray fluorescence spectrometry showed the presence of Rh and Pt atoms in [**1a**]$(NO_3)_4$ and [**1b**]$(NO_3)_4$, and their elemental analytical data were in good agreement with the formula of [Rh(aet)$_3$][Pt(NH$_3$)$_2$](NO$_3$)$_2$. The S-bridged Rh^{III}_2-Pt^{II}_2 tetranuclear structure in [{Pt(NH$_3$)$_2$}$_2${Rh(aet)$_3$}$_2$]$^{4+}$, in which two *fac*(*S*)-[Rh(aet)$_3$] units are linked by two *trans*-[Pt(NH$_3$)$_2$]$^{2+}$ moieties, was established by single-crystal X-ray crystallography for both of [**1a**]$^{4+}$ and [**1b**]$^{4+}$ (vide infra). Thus, it is seen that the reaction of *fac*(*S*)-[Rh(aet)$_3$] with *trans*-[$PtCl_2(NH_3)_2$] proceeds with retention of the *fac*(*S*) configuration. This is in contrast to the previous observation that the reaction of *fac*(*S*)-[Co(aet)$_3$] with $[PdCl_4]^{2-}$ is accompanied by the isomerization to produce an S-bridged $Co^{III}Pd^{II}Co^{III}$ trinuclear complex composed of two *mer(S)*-[Co(aet)$_3$] units, [Pd{Co(aet)$_3$}$_2$]$^{2+}$.[4] Considering the chiral configurations (Δ and Λ) of each *fac*(*S*)-[Rh(aet)$_3$] unit, *meso* (ΔΛ) and *racemic* (ΔΔ/ΛΛ) forms are possible for [{Pt(NH$_3$)$_2$}$_2${Rh(aet)$_3$}$_2$]$^{4+}$. X-ray analysis indicated that [**1a**]$^{4+}$ and [**1b**]$^{4+}$ have the *meso* and *racemic* forms, respectively. This is compatible with the fact that [**1b**]$^{4+}$ was optically resolved into the $(+)^{CD}_{380}$ and $(-)^{CD}_{380}$ isomers, which show CD spectra enantiomeric to each other, by an SP−Sephadex C-25 column chromatography, while [**1a**]$^{4+}$ was not optically resolved. When the Λ isomer of *fac*(*S*)-[Rh(aet)$_3$][10] was reacted with *trans*-[$PtCl_2(NH_3)_2$], instead of the *racemic* one, under the same conditions, only the $(+)^{CD}_{380}$ isomer of [**1b**]$^{4+}$ was formed. Thus, the $(+)^{CD}_{380}$ isomer is assigned to have the ΛΛ configuration, while the $(-)^{CD}_{380}$ one has the ΔΔ configuration. In addition to the *meso*−*racemic* isomerism, another isomerism of *anti*−*syn*, which arises from the relative configuration of two nonbridging groups, are possible for [{Pt(NH$_3$)$_2$}$_2${Rh(aet)$_3$}$_2$]$^{4+}$ (Chart 1). From the X-ray analyses, the two nonbridging thiolato groups in [**1a**]$^{4+}$ and [**1b**]$^{4+}$ were determined to have the *anti* and *syn* configurations, respectively.

Chart 1

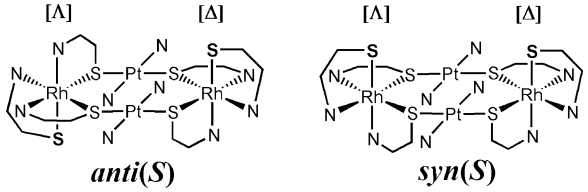

In the ^{13}C NMR spectrum in D_2O, each of [**1a**]$^{4+}$ (ΔΛ-*anti*-[**1**]$^{4+}$) and [**1b**]$^{4+}$ (ΔΔ/ΛΛ-*syn*-[**1**]$^{4+}$) shows three CH_2S carbon signals at a higher magnetic field (δ 31−37) and three CH_2N carbon signals at a lower magnetic field (δ 47−52) due to six aet ligands in the complex. Furthermore, only one ^{195}Pt NMR signal is observed for each of [**1a**]$^{4+}$ and [**1b**]$^{4+}$ in D_2O at similar magnetic fields (δ −2839 for [**1a**]$^{4+}$, δ −2820 for [**1b**]$^{4+}$). These NMR spectral features suggest that the symmetrical S-bridged $Rh^{III}_2Pt^{II}_2$ structures in [**1a**]$^{4+}$ (ΔΛ-*anti*-[**1**]$^{4+}$) and [**1b**]$^{4+}$ (ΔΔ/ΛΛ-*syn*-[**1**]$^{4+}$) found in crystal are retained in solution. Consistent with the isomeric relationship of [**1a**]$^{4+}$ and [**1b**]$^{4+}$, their electronic absorption spectra are very similar to each other, except for a slight deviation in the region of ca. 36−42 × 10^3 cm^{-1}, giving a

(9) (a) Crystal Structure Analysis Package, Rigaku and MSC, 2001. (b) A Computer Program for the Solution and Refinement of Crystal Structures for X-ray Diffraction Data, MAC Science Corporation, Yokohama, 1994.

(10) Konno, T.; Haneishi, K.; Hirotsu, M.; Yamaguchi, T.; Ito, T.; Yoshimura, T. *J. Am. Chem. Soc.* **2003**, *125*, 9244−9245.

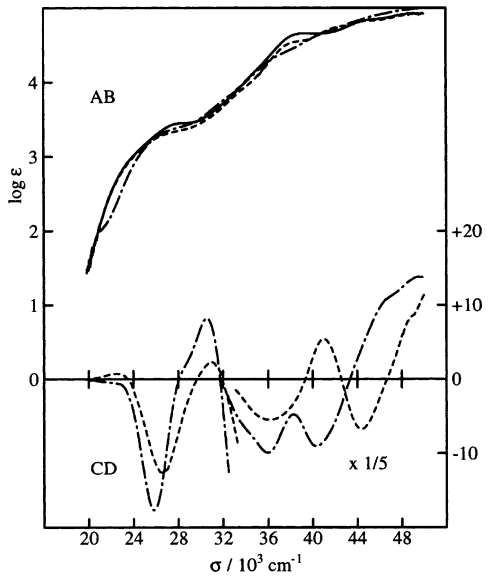

Figure 1. Absorption and CD spectra of ΔΛ-[**1a**]$^{4+}$ (−), $(-)^{CD}_{380}$-ΔΔ-[**1b**]$^{4+}$ (- - -), and $(-)^{CD}_{380}$-ΔΔ-[**3**]$^{5+}$ (-·-) in H_2O.

Table 2. Absorption and CD Spectral Data of [**1a**]$^{4+}$, [**1b**]$^{4+}$, and [**3**]$^{5+}$ in H_2O[a]

abs max: $\sigma/10^3$ cm^{-1} (log ϵ/mol^{-1} dm^3 cm^{-1})		CD extrema: $\sigma/10^3$ cm^{-1} ($\Delta\epsilon$/mol^{-1} dm^3 cm^{-1})	
ΔΛ-*anti*-[{Pt(NH$_3$)$_2$}$_2${Rh(aet)$_3$}$_2$]$^{4+}$ ([**1a**]$^{4+}$)			
23.3	(2.9)^{sh}		
28.0	(3.5)^{sh}		
39.31	(4.66)		
45.0	(4.8)^{sh}		
ΔΔ-*syn*-[{Pt(NH$_3$)$_2$}$_2${Rh(aet)$_3$}$_2$]$^{4+}$ ([**1b**]$^{4+}$)			
23.2	(2.8)^{sh}	22.47	(+0.74)
27.6	(3.3)^{sh}	26.53	(−12.58)
38.5	(4.5)^{sh}	31.06	(+2.29)
42.2	(4.2)^{sh}	35.71	(−25.81)
44.6	(4.8)^{sh}	41.15	(+19.94)
		44.64	(−32.20)
ΔΔ-[Ag{Pt$_2$(H$_2$O)(NH$_3$)$_2$}{Rh(aet)$_3$}$_2$]$^{5+}$ ([**3**]$^{5+}$)			
26.9	(3.3)^{sh}	25.71	(−19.13)
32.0	(3.8)^{sh}	30.40	(+9.09)
36.5	(4.3)^{sh}	35.97	(−46.96)
41.4	(4.7)^{sh}	40.32	(−39.47)

[a] The sh label denotes a shoulder.

d−d transition band at ca. 28 × 10^3 cm^{-1} with a vague shoulder on the lower energy side (ca. 23 × 10^3 cm^{-1}) (Figure 1 and Table 2). Similar two d−d components are also observed in the absorption spectrum of *fac*(*S*)-[Rh(aet)$_3$] at the higher energy side (ca. 26 × 10^3 and 30 × 10^3 cm^{-1}).[7] However, the intensity of the d−d shoulder for each of [**1a**]$^{4+}$ and [**1b**]$^{4+}$ is much lower than that for *fac*(*S*)-[Rh(aet)$_3$]. This is ascribed to the formation of Pt−S bonds, which would diminish an anisotropic π-donor interaction between Rh^{III} and thiolato S atoms.[2d] No significant absorption spectral changes with time were noticed for [**1a**]$^{4+}$ and [**1b**]$^{4+}$ in water at 80 °C for several hours. Thus, the S-bridged $Rh^{III}_2Pt^{II}_2$ structure in [{Pt(NH$_3$)$_2$}$_2${Rh(aet)$_3$}$_2$]$^{4+}$ is fairly stable in solution, which could be ascribed to the intramolecular hydrogen bonding interaction between ammine groups and nonbridging thiolato groups and the Pt···Pt bonding interaction between two square-planar Pt^{II} atoms, together with the relatively strong Pt−S bonds (vide infra).

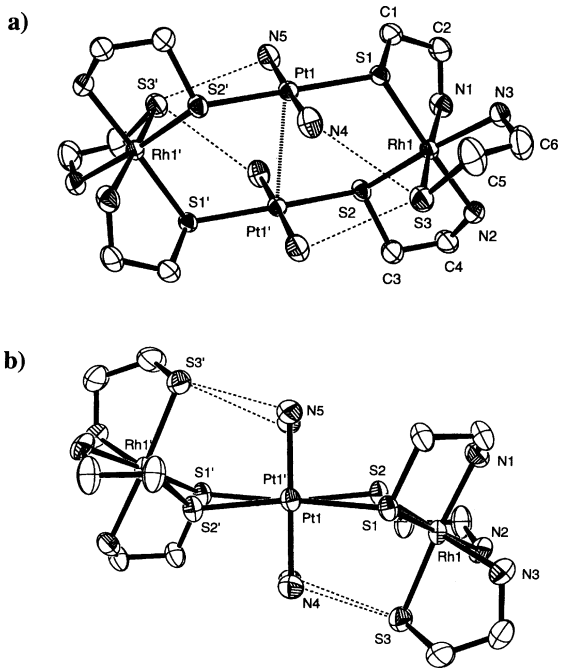

Figure 2. Perspective views of ΔΛ-*anti*-[{Pt(NH$_3$)$_2$}$_2${Rh(aet)$_3$}$_2$]$^{4+}$ ([**1a**]$^{4+}$) with the atomic labeling scheme. Ellipsoids represent 50% probability. Hydrogen atoms are omitted for clarity.

Table 3. Selected Bond Distances and Angles of ΔΛ-*anti*-[{Pt(NH$_3$)$_2$}$_2${Rh(aet)$_3$}$_2$](NO$_3$)$_4$·6H$_2$O ([**1a**](NO$_3$)$_4$·6H$_2$O)

Distances (Å)			
Pt1−S1	2.320(1)	Rh1−S2	2.328(1)
Pt1−S2′	2.325(1)	Rh1−S3	2.333(2)
Pt1−N4	2.043(5)	Rh1−N1	2.124(5)
Pt1−N5	2.055(5)	Rh1−N2	2.108(4)
Rh1−S1	2.335(1)	Rh1−N3	2.127(4)
Angles (deg)			
S1−Pt1−S2′	168.6(1)	S2−Rh1−N2	84.7(1)
S1−Pt1−N4	84.4(1)	S2−Rh1−N3	174.6(1)
S2−Pt1−N5′	94.9(1)	S3−Rh1−N1	174.8(1)
N4−Pt1−N5	176.1(2)	S3−Rh1−N3	85.1(1)
S1−Rh1−S2	96.4(1)	Pt1−S1−Rh1	115.4(1)
S1−Rh1−N1	84.2(1)	Pt1′−S2−Rh1	127.1(1)
S1−Rh1−N2	177.4(2)		

Crystal Structures of ΔΛ-*anti*-[{Pt(NH$_3$)$_2$}$_2${Rh(aet)$_3$}$_2$](NO$_3$)$_4$ ([1a](NO$_3$)$_4$) and ΔΔ/ΛΛ-*syn*-[{Pt(NH$_3$)$_2$}$_2${Rh(aet)$_3$}$_2$](ClO$_4$)$_4$ ([1b](ClO$_4$)$_4$). X-ray structural analysis for [**1a**](NO$_3$)$_4$·6H$_2$O revealed the presence of a discrete complex cation, four NO_3^- anions, and water molecules. The number of nitrate anions implies that the entire complex cation is tetravalent. This is compatible with the observed molar conductivity in water of 501 Ω^{-1} cm^2 mol^{-1}, which is in agreement with that of the 1:4 electrolyte of [{Co$_2$(aet)$_2$}-{Co(aet)$_3$}$_2$](NO$_3$)$_4$ (505 Ω^{-1} cm^2 mol^{-1}).[11] The structure of the entire complex cation [**1a**]$^{4+}$ is shown in Figure 2, and its selected bond distances and angles are listed in Table 3.

The complex cation [**1a**]$^{4+}$ consists of two approximately octahedral [Rh(aet)$_3$] units and two *trans*-[Pt(NH$_3$)$_2$]$^{2+}$ moieties (N−Pt−N = 176.1(2)°), having a crystallographic

(11) Konno, T.; Goto, Y.; Okamoto. K. *Inorg. Chem.* **1997**, *36*, 4992−4997.

center of symmetry at the middle of the Pt−Pt line. The two $[Rh(aet)_3]$ units are spanned by two *trans*-$[Pt(NH_3)_2]^{2+}$ moieties through four of six thiolato S atoms to form an S-bridged $Rh^{III}_2Pt^{II}_2$ tetranuclear structure in $[\{Pt(NH_3)_2\}_2\{Rh(aet)_3\}_2]^{4+}$ that possesses two nonbridging thiolato S atoms (S3 and S3′). Each $[Rh(aet)_3]$ unit has the *fac*(*S*) configuration, like the parental mononuclear *fac*(*S*)-$[Rh(aet)_3]$.[10] The coordination geometry about each Pt^{II} atom is approximately square-planar coordinated by two thiolato S and two ammine N atoms. The two $[PtN_2S_2]$ square-planes face to each other so as to have two parallel N−Pt−N and two parallel S−Pt−S linkages. It is worth noting that the two S−Pt−S angles (168.6(1)°) deviate from linearity toward the center of the Pt−Pt line with a Pt···Pt distance of 3.251(1) Å. This may suggest the presence of a weak bonding interaction between the two square-planar Pt^{II} atom in $[\mathbf{1a}]^{4+}$.[12] Of two possible geometrical configurations, *syn* and *anti*, $[\mathbf{1a}]^{4+}$ adopts the *anti* configuration. The two *fac*(*S*)-$[Rh(aet)_3]$ units have the Δ and Λ configuration to give the *meso* form, and the two bridging S atoms in the Δ- and Λ-$[Rh(aet)_3]$ units are regulated to have the *S* and *R* configurations, respectively. As a result, the two RhN_2S_2 coordination planes, together with two parallel S−Pt−S linkages, yield a flat chairlike conformation, such that each of four NH_3 groups is hydrogen bonded with the adjacent nonbridging thiolato group (N4···S3 = 3.307(6) Å and N5···S3 =3.326(5) Å).[13]

The bond distances and angles about each *fac*(*S*)-$[Rh(aet)_3]$ unit in $[\mathbf{1a}]^{4+}$ (average Rh−S = 2.332(1) Å, Rh−N = 2.120(5) Å, *trans* S−Rh−N = 175.6(1)°) resemble those in $[Pt(bpy)\{Rh(aet)_3\}]^{2+}$ (average Rh−S = 2.318(3) Å, Rh−N = 2.113(9) Å, *trans* S−Rh−N = 172.7(2)°),[14] in which a *fac*(*S*)-$[Rh(aet)_3]$ unit is bound by a *cis*-$[Pt(bpy)]^{2+}$ moiety through two of three thiolato S atoms. However, the S1−Rh1−S2 bridging angle in $[\mathbf{1a}]^{4+}$ (96.4(1)°) is considerably larger than the corresponding angle in $[Pt(bpy)\{Rh(aet)_3\}]^{2+}$ (80.93(9)°). This is understood by the fact that the *fac*(*S*)-$[Rh(aet)_3]$ unit in $[\mathbf{1a}]^{4+}$ binds with two Pt^{II} atoms, while the unit in $[Pt(bpy)\{Rh(aet)_3\}]^{2+}$ chelates to one Pt^{II} atom. The Pt−S bond distances in $[\mathbf{1a}]^{4+}$ (average 2.323(1) Å) are similar to those in $[Pt(bpy)\{Rh(aet)_3\}]^{2+}$ (2.309(3) Å),[14] and the Pt−N distances (average 2.049(5) Å) are essentially the same as the starting *trans*-$[PtCl_2(NH_3)_2]$ (2.05(4) Å).[15]

X-ray analysis for $[\mathbf{1b}](ClO_4)_4\cdot 2H_2O$ indicated the presence of a discrete complex cation, four ClO_4^- anions, and water molecules. The number of perchlorate anions implies that the entire complex cation is tetravalent, which is compatible with the observed molar conductivity in water

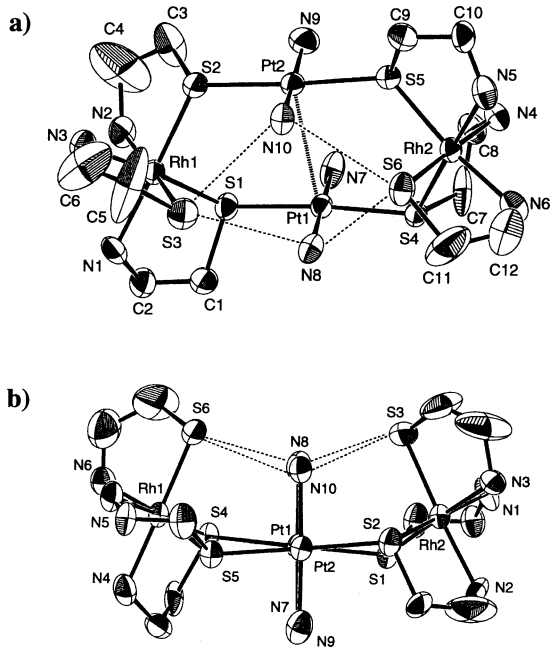

Figure 3. Perspective views of ΔΔ/ΛΛ-*syn*-$[\{Pt(NH_3)_2\}_2\{Rh(aet)_3\}_2]^{4+}$ ($[\mathbf{1b}]^{4+}$) with the atomic labeling scheme. The ΔΔ isomer is selected. Ellipsoids represent 50% probability. Hydrogen atoms are omitted for clarity.

of 509 Ω^{-1} cm^2 mol^{-1}. As shown in Figure 3, the complex cation $[\mathbf{1b}]^{4+}$ consists of two approximately octahedral *fac*(*S*)-$[Rh(aet)_3]$ units that are linked by two parallel *trans*-$[Pt(NH_3)_2]^{2+}$ moieties (average N−Pt−N = 174.3(13)°) to from an S-bridged $Rh^{III}_2Pt^{II}_2$ tetranuclear structure in $[\{Pt(NH_3)_2\}_2\{Rh(aet)_3\}_2]^{4+}$ containing two nonbridging thiolato S atoms (S3 and S6). This S-bridged tetranuclear structure is similar to that found in $[\mathbf{1a}]^{4+}$ (ΔΛ-*anti*-$[\mathbf{1}]^{4+}$). However, the two nonbridging thiolato S atoms in $[\mathbf{1b}]^{4+}$ adopt the *syn* configuration, in contrast to the *anti* configuration for $[\mathbf{1a}]^{4+}$. Furthermore, the two *fac*(*S*)-$[Rh(aet)_3]$ units have the same chiral configuration to give a *racemic* (ΔΔ/ΛΛ) form with four bridging S atoms being fixed to the *S* and *R* configurations for the ΔΔ and ΛΛ isomers, respectively. As a result, in $[\mathbf{1b}]^{4+}$ the two RhN_2S_2 planes, together with two S−Pt−S linkages, form a flat boatlike conformation, such that only two of four NH_3 groups (N8 and N10) are involved in hydrogen bonding with two nonbridging thiolato groups (N8···S3 = 3.30(3) Å, N8···S6 = 3.31(3) Å, N10···S3 = 3.30(3) Å, N10···S6 = 3.37(3) Å). There exists no crystallographycally imposed symmetry in $[\mathbf{1b}]^{4+}$, but an idealized C_2 axis passes through the middle of the Pt−Pt line in parallel with the N−Pt−N linkages. The bond distances and angles around the *fac*(*S*)-$[Rh(aet)_3]$ units (average Rh−S = 2.324(10) Å, Rh−N = 2.12(4) Å, *trans* S−Rh−N = 176.2(9)°) in $[\mathbf{1b}]^{4+}$ are similar to those in $[\mathbf{1a}]^{4+}$ (Table 4). Furthermore, the averaged Pt−S and Pt−N distances in $[\mathbf{1b}]^{4+}$ (average Pt−S = 2.322(9) Å, Pt−N = 2.05(4) Å) are essentially the same as those in $[\mathbf{1a}]^{4+}$ (Pt−S = 2.323(1) Å, Pt−N = 2.049(5) Å). However, it is noticed that the averaged S−Pt−S angle (175.5(4)°) is closer to 180° and the Pt···Pt distance (3.286(2) Å) is slightly longer, compared with the corresponding angle and distance in $[\mathbf{1a}]^{4+}$, suggesting the presence of a weaker Pt···Pt bonding interaction.

(12) (a) Krogmann, K. *Angew. Chem., Int. Ed. Engl.* **1969**, *8*, 35−42. (b) Connick, B. W.; Henling, L. M.; Marsh, R. E. *Acta Crystallogr., Sect. B* **1996**, *52*, 817−822. (c) Pyykkö, P. *Chem. Rev.* **1997**, *97*, 597−636.
(13) (a) Donohue, J. *J. Mol. Biol.* **1969**, *45*, 231−235. (b) Allen, F. H.; Bird, C. M.; Rowland, R. S.; Raithby, P. R. *Acta Crystallogr., Sect. B* **1997**, *53*, 680−695. (c) Desiraju, G. R.; Steiner, T. *The Weak Hydrogen Bond in Structural Chemistry and Biology*; Oxford University Press: New York, 1999; pp 226−230.
(14) Yamada, Y.; Uchida, M.; Miyashita, Y.; Fujisawa, K.; Konno, T.; Okamoto, K. *Bull. Chem. Soc. Jpn.* **2000**, *73*, 913−922.
(15) Milburn, G. H.; Truter, M. R. *J. Chem. Soc. A* **1966**, 1609.

Table 4. Selected Bond Distances and Angles of ΔΔ/ΛΛ-*syn*-[{Pt(NH$_3$)$_2$}$_2$Rh(aet)$_3$}$_2$](ClO$_4$)$_4$·2H$_2$O ([**1b**](ClO$_4$)$_4$·2H$_2$O)

Distances (Å)			
Pt1−S1	2.332(9)	Rh1−S3	2.320(10)
Pt1−S4	2.321(9)	Rh1−N1	2.14(3)
Pt1−N7	2.07(4)	Rh1−N2	2.15(3)
Pt1−N8	2.07(3)	Rh1−N3	2.11(3)
Pt2−S2	2.322(9)	Rh2−S4	2.330(9)
Pt2−S5	2.314(9)	Rh2−S5	2.324(10)
Pt2−N9	2.04(4)	Rh2−S6	2.312(10)
Pt2−N10	2.03(3)	Rh2−N4	2.13(4)
Rh1−S1	2.315(9)	Rh2−N5	2.09(4)
Rh1−S2	2.339(9)	Rh2−N6	2.09(4)
Angles (deg)			
S1−Pt1−S4	174.9(3)	S3−Rh1−N2	176.0(9)
S1−Pt1−N7	84.7(9)	S3−Rh1−N3	85.2(8)
S4−Pt1−N8	94.8(9)	S4−Rh2−S5	97.5(4)
N7−Pt1−N8	174.8(13)	S4−Rh2−N4	85.5(9)
S2−Pt2−S5	176.0(4)	S4−Rh2−N5	178.0(9)
S2−Pt2−N9	95.2(10)	S5−Rh2−N5	83.7(9)
S5−Pt2−N10	93.4(9)	S5−Rh2−N6	172.3(9)
N9−Pt2−N10	173.8(12)	S6−Rh2−N4	178.0(9)
S1−Rh1−S2	96.8(4)	S6−Rh2−N6	86.2(10)
S1−Rh1−N1	84.5(9)	Pt1−S1−Rh1	125.9(4)
S1−Rh1−N3	174.7(9)	Pt2−S2−Rh1	116.1(4)
S2−Rh1−N1	178.3(9)	Pt1−S4−Rh2	115.9(4)
S2−Rh1−N2	85.4(9)	Pt2−S5−Rh2	127.1(4)

Synthesis and Characterization of {[Ag{Pt(NH$_3$)$_2$}$_2$-{Rh(aet)$_3$}$_2$]$^{5+}$}$_n$ ([2]$^{5+}$) and [Ag{Pt$_2$(H$_2$O)(NH$_3$)$_2$}{Rh-(aet)$_3$}$_2$]$^{5+}$ ([3]$^{5+}$). Treatment of an aqueous solution of [**1a**](NO$_3$)$_4$ with one molar equiv of AgClO$_4$, followed by the addition of aqueous NaClO$_4$, gave yellow crystals of [**2**]-(ClO$_4$)$_5$. Compound [**2**](ClO$_4$)$_5$ is poorly soluble in water, unlike the parental [**1a**](NO$_3$)$_4$. X-ray fluorescence spectrometry indicated the presence of Rh, Pt, and Ag atoms in [**2**](ClO$_4$)$_5$, and its elemental analytical data are in good agreement with the formula of [{Pt(NH$_3$)$_2$}$_2$Rh(aet)$_3$}$_2$]-(ClO$_4$)$_4$·AgClO$_4$. In addition, the diffuse reflection spectrum of [**2**](ClO$_4$)$_5$ in the solid state is very similar to that of [**1a**]-(NO$_3$)$_4$, showing a shoulder at ca. 355 nm and a broad intense peak at 260 nm. These results imply that [**2**]$^{5+}$ consists of [{Pt(NH$_3$)$_2$}$_2$Rh(aet)$_3$}$_2$]$^{4+}$ and Ag^{I} in a 1:1 ratio. The one-dimensional {Rh$^{III}_2$Pt$^{II}_2$Ag^{I}}$_n$ polymeric structure in {[Ag-{Pt(NH$_3$)$_2$}$_2$Rh(aet)$_3$}$_2$]$^{5+}$}$_n$, in which ΔΛ-*anti*-[{Pt(NH$_3$)$_2$}$_2$-{Rh(aet)$_3$}$_2$]$^{4+}$ units are alternately linked by linear Ag^{I} atoms, was established by the X-ray analysis for [**2**](ClO$_4$)$_5$ (vide infra). Thus, it is seen that [**1a**]$^{4+}$ (ΔΛ-*anti*-[**1**]$^{4+}$) reacts with Ag^{I} through two nonbridging thiolato groups, retaining the S-bridged Rh$^{III}_2$Pt$^{II}_2$ tetranuclear structure having the ΔΛ-*anti* configuration.

The corresponding 1:1 reaction of [**1b**](NO$_3$)$_4$ with AgNO$_3$ in water produced yellow crystals of [**3**](NO$_3$)$_5$, which are easily soluble in water. While the presence of Rh, Pt, and Ag atoms in [**3**](NO$_3$)$_5$ was confirmed by X-ray fluorescence spectrometry, its elemental analytical data do not match with the formula of the 1:1 adduct of [{Pt(NH$_3$)}$_2$Rh(aet)$_3$}$_2$]-(NO$_3$)$_4$·AgNO$_3$, having a N/C value of ca. 13/12 that is smaller than the value of 15/12 expected for this 1:1 adduct. In the ^{195}Pt NMR spectrum in D$_2$O, [**3**]$^{5+}$ exhibits a sharp signal as does the parental [**1b**]$^{4+}$, but its chemical shift is located at a magnetic field (δ −2885) higher than that for [**1b**]$^{4+}$ (δ −2820). This is suggestive of the difference in coordination environment around Pt^{II} atoms between [**3**]$^{5+}$ and [**1b**]$^{4+}$. X-ray analysis demonstrated that [**3**]$^{5+}$ has a discrete Rh$^{III}_2$Pt$^{II}_2$Ag^{I} pentanuclear structure in [Ag{Pt$_2$(H$_2$O)-(NH$_3$)$_2$}{Rh(aet)$_3$}$_2$]$^{5+}$, in which two Δ- or Λ-*fac*(*S*)-[Rh-(aet)$_3$] units are linked by an O-bridged [Pt$^{II}_2$(μ-H$_2$O)-(NH$_3$)$_2$]$^{4+}$ moiety, together with a linear Ag^{I} atom (vide infra). Thus, two of four NH$_3$ molecules bound to Pt^{II} centers in [**1b**]$^{4+}$ (ΔΔ/ΛΛ-*syn*-[**1**]$^{4+}$) are replaced by one bridging H$_2$O molecule in the course of the reaction, while the ΔΔ/ΛΛ-*syn* configuration is retained. Molecular model examinations reveal that the linkage of two nonbridging thiolato groups in [**1b**]$^{4+}$ with Ag^{I} causes a serious nonbonding interaction between two NH$_3$ groups. The ^{13}C NMR spectrum of [**3**]$^{5+}$ in D$_2$O shows only three CH$_2$S and three CH$_2$N methylene carbon signals for six aet ligands in the complex, consistent with the C_2-symmetrical S-bridged structure found in crystal. Complex [**3**]$^{5+}$ was optically resolved into the $(+)^{CD}_{380}$ and $(-)^{CD}_{380}$ isomers, which show CD spectra enantiomeric to each other, by an SP−Sephadex C-25 column chromatography. When the $(-)^{CD}_{380}$-ΔΔ isomer of [**1b**]$^{4+}$ was reacted with Ag^{I}, instead of the racemate of [**1b**]$^{4+}$, only the $(-)^{CD}_{380}$ isomer of [**3**]$^{5+}$ was obtained. Thus, the $(-)^{CD}_{380}$ isomer of [**3**]$^{5+}$ is confidently assigned to have the ΔΔ configuration, while the $(+)^{CD}_{380}$ isomer has the ΛΛ configuration. The CD spectral curve of $(-)^{CD}_{380}$-ΔΔ-[**3**]$^{5+}$ deviates significantly from that of $(-)^{CD}_{380}$-ΔΔ-[**1b**]$^{4+}$ over the whole region, although [**3**]$^{5+}$ show an absorption spectrum similar to that of [**1b**]$^{4+}$, except the disappearance of the d−d shoulder owing to the absence of nonbridging thiolato donors in [**3**]$^{5+}$ (Figure 1 and Table 2). The two thiolato S atoms in [**3**]$^{5+}$, which become asymmetric on bridging with Ag^{I}, seem to be responsible for the CD spectral deviation.[4]

Crystal Structures of {[Ag{Pt(NH$_3$)$_2$}$_2$-{Rh(aet)$_3$}$_2$]-(ClO$_4$)$_5$}$_n$ ([2](ClO$_4$)$_5$) and [Ag{Pt$_2$(μ-H$_2$O)(NH$_3$)$_2$}{Rh-(aet)$_3$}$_2$](NO$_3$)$_5$ ([3](NO$_3$)$_5$). X-ray analysis indicated that in the asymmetric unit [**2**](ClO$_4$)$_5$·3H$_2$O contains a *fac*(*S*)-[Rh(aet)$_3$] unit that is bound by a [Pt(NH$_3$)$_2$]$^{2+}$ moiety and a Ag^{I} atom, besides 2.5 ClO$_4^-$ anions and water molecules. As shown in Figure 4, the entire complex-cation consists of [{Pt(NH$_3$)$_2$}$_2$Rh(aet)$_3$}$_2$]$^{4+}$ tetranuclear units and Ag^{I} atoms in a 1:1 ratio, which are alternately linked with each other through sulfur bridges to form a (Rh$^{III}_2$Pt$^{II}_2$Ag^{I})$_n$ one-dimensional chain structure in {[Ag{Pt(NH$_3$)$_2$}$_2$Rh-(aet)$_3$}$_2$]$^{5+}$}$_n$. Each [{Pt(NH$_3$)$_2$}$_2$Rh(aet)$_3$}$_2$]$^{4+}$ tetranuclear unit adopts the ΔΛ-*anti* configuration, as does the parental [**1a**]$^{4+}$. The three bridging S atoms of each of the Δ- and Λ-[Rh(aet)$_3$] units are regulated to have the *S* and *R* configurations, respectively, leading to an achiral one-dimensional chain. The bond distances and angles concerning the [{Pt(NH$_3$)$_2$}$_2$Rh(aet)$_3$}$_2$]$^{4+}$ tetranuclear unit in [**2**]$^{5+}$ (average Rh−S = 2.327(5) Å, Rh−N = 2.10(1) Å, Pt−S = 2.311(4) Å), Pt−N = 2.06(1) Å) are very similar to those in the parental [**1a**]$^{4+}$ (Table 5). However, the S3···N5′ and S3′···N5 distances (3.47(1) Å) in [**2**]$^{5+}$ are considerably longer than the corresponding distances in the parental [**1a**]$^{4+}$, though the S3···N4 and S3′···N4′ distances (3.30(1) Å) are comparable. This indicates that the intramolecular NH···S

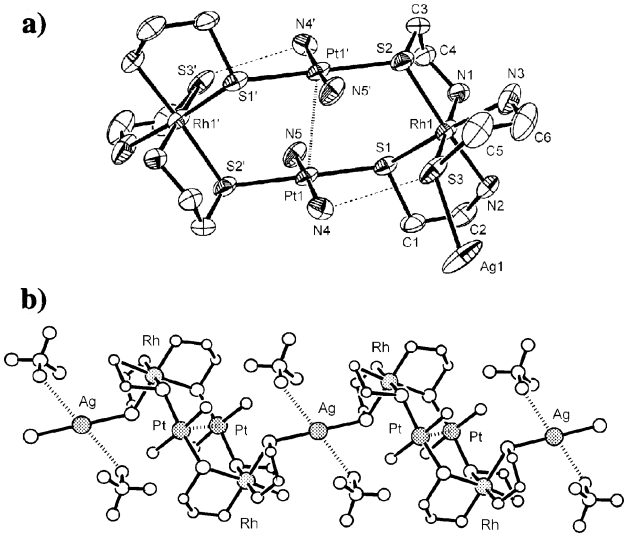

Figure 4. Perspective views of (a) the $Rh^{III}Pt^{II}$ tetranuclear unit bound by Ag^{I} atom in $\{[Ag\{[Pt(NH_3)_2]_2[Rh(aet)_3]_2\}]^{5+}\}_n$ ([**2**]$^{5+}$) and (b) its one-dimensional chain structure contacted with perchlorate anions. Hydrogen atoms are omitted for clarity.

Table 5. Selected Bond Distances and Angles of $[Ag\{[Pt(NH_3)_2]_2[Rh(aet)_3]_2\}](ClO_4)_5\cdot 3H_2O$ ([**2**]$(ClO_4)_5\cdot 3H_2O$)

Distances (Å)			
Pt1−S1	2.308(4)	Rh1−S2	2.342(4)
Pt1−S2′	2.313(4)	Rh1−S3	2.331(5)
Pt1−N4	2.06(1)	Rh1−N1	2.09(1)
Pt1−N5	2.06(1)	Rh1−N2	2.10(1)
Ag1−S3	2.447(4)	Rh1−N3	2.10(1)
Rh1−S1	2.307(4)		
Angles (deg)			
S1−Pt1−S2′	169.7(1)	S2−Rh1−N1	175.9(4)
S1−Pt1−N4	94.0(4)	S2−Rh1−N2	85.4(3)
S2−Pt1−N5′	85.0(4)	S3−Rh1−N2	176.3(3)
N4−Pt1−N5	173.1(5)	S3−Rh1−N3	85.3(5)
S3−Ag−S3′	180.0(2)	Pt1−S1−Rh1	128.3(2)
S1−Rh1−S2	96.6(1)	Pt1−S2−Rh1′	116.3(2)
S1−Rh1−N1	85.0(4)	Ag1−S3−Rh1	125.4(2)
S1−Rh1−N3	174.9(4)		

hydrogen bonding interaction in the parental [**1a**]$^{4+}$ is weakened because of the coordination of the nonbridging thiolato S atoms toward Ag^{I} atoms. In addition, in [**2**]$^{5+}$ the Pt···Pt distance (3.271(1) Å) is slightly longer and the S−Pt−S angle (169.7(1)°) is slightly larger, compared with those in [**1a**]$^{4+}$, which may be related to the weaker NH···S interactions in [**2**]$^{5+}$. Each Ag^{I} atom in [**2**]$^{5+}$ has a perfect linear geometry coordinated by two S atoms from two different tetranuclear units, as evidenced by a crystallographic inversion center located on it. The Ag−S bond distances (2.447(4) Å) in [**2**]$^{5+}$ are longer than those in $[Ag_3\{Rh(aet)_3\}_2]^{3+}$ (average 2.376(6) Å) and $[Ag_3\{Co(aet)_3\}_2]^{3+}$ (average 2.378(8) Å), in which two octahedral *fac*(*S*)-[M(aet)$_3$] units (M = Co^{III}, Rh^{III}) are linked by three linear Ag^{I} atoms.[16] Of note is the presence of close contact of two ClO_4^- anions with each Ag^{I} atom (Ag···O = 2.81(2) Å) in [**2**]$^{5+}$, which seems to be responsible for the longer Ag−S bonds.

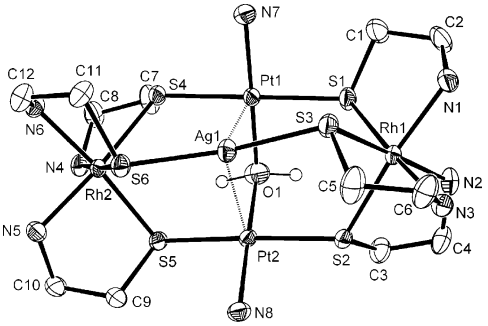

Figure 5. A perspective view of $[Ag\{Pt_2(\mu\text{-}H_2O)(NH_3)_2\}\{Rh(aet)_3\}_2]^{5+}$ ([**3**]$^{5+}$) with the atomic labeling scheme. The ΔΔ isomers are selected. Ellipsoids represent 50% probability. Hydrogen atoms, except for a bridging water molecule, are omitted for clarity.

X-ray structural analysis for [**3**]$(NO_3)_5\cdot 10H_2O$ showed the presence of a discrete complex cation, NO_3^- anions, and water molecules. While the nitrate anions in the asymmetric unit of [**3**]$(NO_3)_5\cdot 10H_2O$ could not be definitely determined because of their severe disorder, the elemental analytical result implies that a complex cation and nitrate anions exist in a 1:5 ratio. This is compatible with the observed molar conductivity in water of 601 Ω^{-1} cm^2 mol^{-1}, which is in agreement with that of the 1:5 electrolyte of $[Ag\{Co(aet)(en)_2\}_2](NO_3)_5$ (605 Ω^{-1} cm^2 mol^{-1}).[2b] As shown in Figure 5, the complex cation [**3**]$^{5+}$ consists of two *fac*(*S*)-[Rh(aet)$_3$] octahedral units that are spanned by one Ag^{I} and two Pt^{II} atoms to form an S-bridged $Rh^{III}_2Pt^{II}_2Ag^{I}$ pentanuclear structure in $[Ag\{Pt_2(\mu\text{-}H_2O)(NH_3)_2\}\{Rh(aet)_3\}_2]^{5+}$, in which five metals form a trigonal-bipyramid. Each of the two Pt^{II} atoms is planarly coordinated by two thiolato S atoms from two *fac*(*S*)-[Rh(aet)$_3$] units, one N atom, and one water O atom that bridges two Pt^{II} centers (average S−Pt−S = 175.8(1)°, N−Pt−O = 177.1(1)°). It is interesting to note that this seems to be the first example of a structurally characterized metal-organic compound involving a Pt^{II}−H_2O−Pt^{II} fragment, although a large number of diplatinum(II) structures bridged by a hydroxide ion have been presented in the Cambridge Structural Database. The two *fac*(*S*)-[Rh(aet)$_3$] units in [**3**]$^{5+}$ have the same chiral configuration to give the *racemic* (ΔΔ/ΛΛ) form, like the two units in the parental [**1b**]$^{4+}$ (ΔΔ/ΛΛ-*syn*-[**1**]$^{4+}$). The coordination geometry about the Ag^{I} atom in [**3**]$^{5+}$ is deviated considerably from linearity (S−Ag−S = 161.9(1)°) toward the middle of the Pt−Pt line having two Ag···Pt distances of 2.962(2) Å and 2.958(1) Å. This suggests that an appreciable bonding interaction exists between Pt^{II} and Ag^{I} atoms in [**3**]$^{5+}$.[17] The Pt···Pt distance in [**3**]$^{5+}$ (3.421(2) Å) is much longer than that in the parental [**1b**]$^{4+}$, indicative of the absence of a Pt−Pt bond.[12] In [**3**]$^{5+}$, there is no crystallographycally imposed symmetry, but an idealized C_2 axis passes through the Ag and O atoms.

The bond distances and angles about each *fac*(*S*)-[Rh(aet)$_3$] unit in [**3**]$^{5+}$ (average Rh−S = 2.326(2) Å, Rh−N = 2.114(2) Å, *trans* S−Rh−N = 175.3(1)°) are essentially the

(16) (a) Konno, T.; Okamoto, K. *Inorg. Chem.* **1997**, *36*, 1403−1406. (b) Konno, T.; Tokuda, K.; Suzuki, T.; Okamoto, K. *Bull. Chem. Soc. Jpn.* **1998**, *71*, 1049−1054.

(17) (a) Rochon, F. D.; Melanson, R. *Acta Crystallogr., Sect. A* **1988**, *44*, 474−477. (b) Yamaguchi, T.; Yamazaki, F.; Ito, T. *J. Chem. Soc., Dalton Trans.* **1999**, 273−274.

Table 6. Selected Bond Distances and Angles of $[Ag\{Pt_2(H_2O)(NH_3)_2\}\{Rh(aet)_3\}_2](NO_3)_5\cdot 10H_2O$ ($[\mathbf{3}](NO_3)_5\cdot 10H_2O$)

Distances (Å)			
Pt1−S1	2.313(2)	Rh1−S2	2.321(2)
Pt1−S4	2.313(2)	Rh1−S3	2.331(1)
Pt1−N7	2.064(2)	Rh1−N1	2.113(2)
Pt1−O1	2.034(2)	Rh1−N2	2.115(2)
Pt2−S2	2.309(2)	Rh1−N3	2.110(2)
Pt2−S5	2.306(2)	Rh2−S4	2.325(1)
Pt2−N8	2.065(2)	Rh2−S5	2.327(2)
Pt2−O1	2.039(2)	Rh2−S6	2.326(1)
Ag1−S3	2.398(2)	Rh2−N4	2.125(2)
Ag1−S6	2.400(2)	Rh2−N5	2.111(2)
Rh1−S1	2.325(1)	Rh2−N6	2.109(2)
Angles (deg)			
S1−Pt1−S4	175.8(1)	S3−Rh1−N3	85.6(1)
S1−Pt1−N7	94.7(1)	S4−Rh2−S5	99.3(1)
S1−Pt1−O1	86.2(1)	S4−Rh2−N4	85.1(1)
N7−Pt1−O1	177.3(1)	S4−Rh2−N5	174.9(1)
S2−Pt2−S5	175.7(1)	S5−Rh2−N5	85.5(1)
S2−Pt2−N8	86.5(1)	S5−Rh2−N6	173.8(1)
S5−Pt2−O1	85.8(1)	S6−Rh2−N4	176.5(1)
N8−Pt2−O1	176.8(1)	S6−Rh2−N6	86.5(1)
S3−Ag−S6	161.9(1)	Pt1−S1−Rh1	116.0(1)
S1−Rh1−S2	96.8(1)	Pt2−S2−Rh1	122.1(1)
S1−Rh1−N1	85.8(1)	Ag1−S3−Rh1	110.3(1)
S1−Rh1−N3	175.6(1)	Pt1−S4−Rh2	122.5(1)
S2−Rh1−N1	174.2(1)	Pt2−S5−Rh2	116.9(1)
S2−Rh1−N2	85.0(1)	Ag1−S6−Rh2	109.7(1)
S3−Rh1−N2	176.8(1)	Pt1−O1−Pt2	114.2(1)

same as those found in the parental $[\mathbf{1b}]^{4+}$ (Table 6). Furthermore, no significant difference is observed for the Pt−S distances between $[\mathbf{3}]^{5+}$ (average 2.310(2) Å) and $[\mathbf{1b}]^{4+}$. The Ag−S bond distances (average 2.399(2) Å) in $[\mathbf{3}]^{5+}$ are similar to those in $[Ag_3\{M(aet)_3\}_2]^{3+}$ (M = Co^{III}, Rh^{III}),[16] and thus shorter than those in $[\mathbf{2}]^{5+}$. Compatible with the fact that the bridging O species in $[\mathbf{3}]^{5+}$ is a water molecule,[18] the Pt−O bond distances (average 2.037(8) Å) in $[\mathbf{3}]^{5+}$ are comparable with that found in the mononuclear *cis*-$[Pt(NH_3)_2$(1-methylcytosine)$(H_2O)]$ (Pt−O = 2.052(8) Å).[19] On the other hand, the Pt−O bonds in $[\mathbf{3}]^{5+}$ are longer than those in $[cis\text{-}\{Pt(NH_3)_2\}_2(\mu\text{-OH})$(triazolate)$](NO_3)_2$, in which two Pt^{II} centers are bridged by a hydroxo O atom (average Pt−O = 2.020(5) Å).[20]

Construction and Stereochemistry of S-Bridged Structures Based on *fac*(*S*)-[Rh(aet)$_3$]. The formation of an S-bridged $Rh^{III}_2Pt^{II}_2$ tetranuclear structure in $[\{Pt(NH_3)_2\}_2\{Rh(aet)_3\}_2]^{4+}$ ($[\mathbf{1}]^{4+}$) was achieved by the 1:1 reaction of *fac*(*S*)-[Rh(aet)$_3$] with *trans*-$[PtCl_2(NH_3)_2]$ at a low temperature (0 °C). On the other hand, the reaction at a relatively high temperature caused the release of NH_3 molecules to give uncharacterized polymeric species that are adsorbed on the top of the SP−Sephadex C-25 column, like the reaction solutions obtained from *fac*(*S*)-[Rh(aet)$_3$] and $[PdCl_4]^{2-}$ or $[PtCl_4]^{2-}$.[5] Attempts to prepare the analogous S-bridged $Rh^{III}_2Pd^{II}_2$ complex, $[\{Pd(NH_3)_2\}_2\{Rh(aet)_3\}_2]^{4+}$, by the reaction of *fac*(*S*)-[Rh(aet)$_3$] with $[PdCl_2(NH_3)_2]$ were unsuccessful even at 0 °C, leading to the release of NH_3 molecules owing to the weaker Pd−NH_3 bonds. In addition, similar reactions of *fac*(*S*)-[Rh(aet)$_3$] with M = Ag^I and Au^I do not give the related $Rh^{III}_2M_2$ tetranuclear complexes having two nonbridging thiolato groups, $[M_2\{Rh(aet)_3\}_2]^{4+}$, but produced $[Ag_5\{Rh(aet)_3\}_4]^{5+}$ and $[Au_3\{Rh(aet)_3\}_2]^{3+}$, respectively, in which all the thiolato groups in *fac*(*S*)-[Rh(aet)$_3$] units are bridged by Ag^I or Au^I ions.[16,21] Thus, the presence of two *trans* NH_3 groups in the bridging metal unit is essential for the linkage of two *fac*(*S*)-[Rh(aet)$_3$] units so as to reserve two nonbridging thiolato groups.

Four stereoisomers, ΔΛ-*anti*, ΔΔ/ΛΛ-*anti*, ΔΛ-*syn*, and ΔΔ/ΛΛ-*syn*, are possible for $[\{Pt(NH_3)_2\}_2\{Rh(aet)_3\}_2]^{4+}$ ($[\mathbf{1}]^{4+}$), based on the combination of chiral configurations (Δ and Λ) of two *fac*(*S*)-[Rh(aet)$_3$] units and geometrical configurations (*syn* and *anti*) of two nonbridging thiolato S atoms. However, only the ΔΛ-*anti* ($[\mathbf{1a}]^{4+}$) and ΔΔ/ΛΛ-*syn* ($[\mathbf{1b}]^{4+}$) isomers are formed for $[\mathbf{1}]^{4+}$, which was confirmed by an SP−Sephadex C-25 column chromatography of the reaction solution, together with their single-crystal X-ray analyses. Molecular model examinations point out that an unfavorable nonbonding interaction exists between NH_3 molecules and aet chelate rings in $[\mathbf{1}]^{4+}$ when the ΔΔ/ΛΛ and ΔΛ isomers adopt the *anti* and *syn* configurations, respectively. Compatible with this, the use of Λ-*fac*(*S*)-[Rh(aet)$_3$] for the reaction with $[PtCl_2(NH_3)_2]$, instead of the *racemic fac*(*S*)-[Rh(aet)$_3$], led to the stereoselective formation of the ΛΛ-*syn* isomer.

Both of the ΔΛ-*anti*- and ΔΔ/ΛΛ-*syn* isomers of $[\mathbf{1}]^{4+}$ readily reacted with Ag^I through two nonbridging thiolato groups to produce a one-dimensional $\{Rh^{III}_2Pt^{II}_2Ag^I\}_n$ chain structure in $\{[Ag\{Pt(NH_3)_2\}_2\{Rh(aet)_3\}_2]^{5+}\}_n$ ($[\mathbf{2}]^{5+}$) and a discrete $Rh^{III}_2Pt^{II}_2Ag^I$ pentanuclear structure in $[Ag\{Pt_2(\mu\text{-}H_2O)(NH_3)_2\}\{Rh(aet)_3\}_2]^{5+}$ ($[\mathbf{3}]^{5+}$), respectively. This result clearly indicates that $[\mathbf{1}]^{4+}$ could be used as a multinuclear precursor for the construction of a variety of S-bridged hetellometallic aggregates, the overall structures of which are changed by the stereoisomerism of $[\mathbf{1}]^{4+}$. While the reaction of ΔΛ-*anti*-$[\mathbf{1}]^{4+}$ with Ag^I proceeded with retention of its $Rh^{III}_2Pt^{II}_2$ tetranuclear structure, the reaction of the ΔΔ/ΛΛ-*syn* isomer was accompanied by the conversion of two *trans*-$[Pt(NH_3)_2]^{2+}$ moiety into an O-bridged $[Pt_2(\mu\text{-}H_2O)(NH_3)_2]^{4+}$ dinuclear moiety because of the steric demand. Previously, we have shown that the related S-bridged trinuclear complexes with two nonbridging thiolato groups, ΔΔ/ΛΛ-*syn*-$[Pd\{Co(aet)_3\}_2]^{2+}$, in which two *mer*(*S*)-[Co(aet)$_3$] units are linked by a square-planar Pd^{II} ion, also react with linear M = Ag^I, Au^I ions. However, these reactions produced S-bridged $Co^{III}_4Pd^{II}_2M_2$ octanuclear complexes, $[M_2\{Pd\{Co(aet)_3\}_2\}_2]^{6+}$, in which two $Co^{III}Pd^{II}Co^{III}$ trinuclear units are connected by two Ag^I or Au^I ions in a cyclic form.[4] Accordingly, the overall structures of S-bridged heterometallic aggregates based on [M(aet)$_3$] are controlled not only by a combination of the *meso*−*racemic* and *syn*−*anti* isomerisms of a multinuclear precursor, but also by the *fac*(*S*)−*mer*(*S*) isomerism of the constitutional [M(aet)$_3$] unit, which determines the directionality of lone pairs on non-

(18) The O−H distances (1.05 Å and 1.10 Å) and the H−O−H angle (118.9°) concerning the bridging O atom in $[\mathbf{3}]^{5+}$ are compatible with those expected for a water molecule.

(19) Britten, J. F.; Lippert, B.; Lock, C. J. L.; Pilon, P. *Inorg. Chem.* **1982**, *21*, 1936−1941.

(20) Komeda, S.; Lutz, M.; Spek A. L.; Chikuma, M.; Reedijk, J. *Inorg. Chem.* **2000**, *39*, 4230−4236.

(21) Konno, T.; Tokuda, K.; Abe, T.; Hirotsu, M. *Mol. Cryst. Liq. Cryst.* **2000**, *342*, 45−50.

bridging thiolato S atoms available for binding with additional metal centers.

Conclusion

In this study, the linkage of two *fac*(*S*)-[Rh(aet)$_3$] molecules with transition metal ions was achieved by the reaction with *trans*-[PtCl$_2$(NH$_3$)$_2$] to produce an S-bridged $Rh^{III}_2Pt^{II}_2$ tetranuclear complex having two nonbridging thiolato groups, $[\{Pt(NH_3)_2\}_2\{Rh(aet)_3\}_2]^{4+}$ ([**1**]$^{4+}$), which forms only the ΔΛ-*anti* and ΔΔ/ΛΛ-*syn* stereoisomers. This result first shows that the *trans*-[Pt(NH$_3$)$_2$]$^{2+}$ unit could function as an effective, bulky linker for the stereoselective construction of S-bridged polynuclear structures comprising of thiolato complex octahedra. The ΔΛ-*anti* and ΔΔ/ΛΛ-*syn* isomers of [**1**]$^{4+}$ reacted readily with Ag^I to afford a 1D $\{Rh^{III}_2Pt^{II}_2Ag^I\}_n$ polymeric and a discrete $Rh^{III}_2Pt^{II}_2Ag^I$ pentanuclear complexes, respectively, which is indicative of the utility of [**1**]$^{4+}$ as a multinuclear metalloligand for the construction of metallo-aggregates consisting of transition metal centers with different coordination geometries and oxidation states. Finally, the present result points out that heterometallic supramolecular species exhibiting unique structures and properties could be created only from thiolato metal complexes with simple aminothiolate ligands through the stepwise combinations with transition metal ions that are appropriately selected. The construction of other polynuclear and polymeric structures based on ΔΛ-*anti*- and ΔΔ/ΛΛ-*syn*-[**1**]$^{4+}$ in combination with other transition metal ions, together with the creation of novel S-bridged multinuclear complexes having nonbridging thiolato groups by the introduction of *trans*-[Pt(NH$_2$R)$_2$]$^{2+}$ linkers, is currently under way.

Acknowledgment. This work was partially supported by Grant-in-Aid for Scientific Research on Priority Areas (No. 16033235) from Ministry of Education, Culture, Sports, Science and Technology. One of the authors (Y. Chikamoto) expresses his special thanks for the center of excellence (21COE) program "Creation of Integrated EcoChemistry of Osaka University".

Supporting Information Available: X-ray crystallographic files, in CIF format, for the structure determinations of [**1a**](NO$_3$)$_4$·6H$_2$O, [**1b**](ClO$_4$)$_4$·2H$_2$O, [**2**](ClO$_4$)$_5$·3H$_2$O, and [**3**](NO$_3$)$_5$·10H$_2$O. This material is available free of charge via the Internet at http://pubs.acs.org.

IC048680K